

## H13-135

## CFD SIMULATIONS OF DISPERSION AROUND OBSTACLES OF DIFFERENT SHAPES

S. Andronopoulos<sup>1</sup>, I. Mavroidis<sup>2</sup>, A. Venetsanos<sup>1</sup>, J.G. Bartzis<sup>1,3</sup><sup>1</sup> Environmental Research Laboratory/INT-RP, NCSR Demokritos, Aghia Paraskevi Attikis, Greece<sup>2</sup> Hellenic Open University, Patras, Greece<sup>3</sup> University of Western Macedonia, Department of Mechanical Engineering, Kozani, Greece

**Abstract:** This paper presents computational simulations of atmospheric dispersion experiments conducted around isolated obstacles in a wind tunnel. The computational tool used for the simulations was the code ADREA-HF, which was especially developed for the simulation of the dispersion of positively or negatively buoyant gases in complicated geometries. The wind tunnel experiments simulated involve a cube normal to the flow and a right circular cylinder. In addition to the different obstacle shapes, different gas source locations, using a neutrally buoyant gas, have been tested in the experiments: 2 obstacle heights upwind, at the upwind face, on the roof and at the downwind face of the obstacle. In all cases mean concentrations and standard deviation of concentrations have been measured at several locations downwind of the obstacle, at half the obstacle height and on the ground. The main purpose of the computational simulations presented here is to evaluate the model's performance. Concentrations and concentration fluctuations for both gases are calculated by the model and compared with the experimental results. The results show a good level of agreement between calculated and measured concentrations and concentration fluctuations. The detailed spatial results that the CFD model produces, give the opportunity to study also the plume contours and concentration patterns due to the different obstacle shapes and gas source locations.

**Key words:** atmospheric dispersion; cube; circular cylinder; wake; model evaluation; concentration fluctuations; source location..

## INTRODUCTION

Although in real situations involving dispersion of atmospheric pollutants in urban areas there is a complex interaction between pollutant plumes and groups of buildings and other obstacles, the study of flow and dispersion around isolated simple structures is very useful for detecting the fundamental characteristics of building influenced dispersion and for investigating routine or accidental releases of airborne hazardous or radioactive substances, since these are usually released near industrial installations or other structures. Close to the source, where the interaction between the plume and single structures dominates the plume path and its dispersion, field trials and wind tunnel modelling studies are often used, in order to improve the understanding of the physical processes involved and provide the necessary information to develop and validate mathematical modelling approaches as a practical tool. The presence of buildings and the interaction between the approach flow and the building wakes leads to the possibility of material released in the vicinity of a building becoming entrained in these local flows instead of passing around the region influenced by the building.

The main characteristics of the flow around a cubical obstacle normal to the flow are described in detail by Hosker (1984). As the mean flow approaches the obstacle, it decelerates longitudinally and accelerates laterally and vertically to pass around it. One or more standing horizontally oriented vortices are generated near the ground upwind of the obstacle, which wrap around the sides of the obstacle to trail off downwind as a counter rotating vortex pair, the so-called horseshoe vortex. This vortex has the ability to entrain material from plumes impinging on the obstacle and to carry contaminants laterally around (rather than over) an obstacle, while keeping them close to the ground. The flow separates at the sharp edges on the upwind face of the obstacle and then (in a turbulent sheared approach flow) usually reattaches on the top and the sides of the obstacle and separates again at the downwind edges to reattach on the ground further downwind. The flow around a vertically mounted three dimensional cylinder has certain similarities with the flow around a rectangular obstacle normal to the flow, since a horseshoe vortex is similarly generated near the ground upwind of the cylinder. The recirculation region behind finite length cylinders depends to some extent on the diameter to height ratio. The recirculation region behind rounded obstacles also depends on the exact location of the flow separation from the obstacle since this is determined by aerodynamic force balances rather than by geometry alone. The main parameters affecting separation are the Reynolds number and the approach flow turbulence (Hosker, 1984).

The present work aims at calculating mean concentrations and, especially, concentration fluctuations downwind of single obstacles for different source locations, in order to compare it with detailed results from wind tunnel experiments and to evaluate the performance of the ADREA-HF model in the prediction of mean concentrations as well as concentration fluctuations in obstacle-obstructed flows. The use of CFD models in security-related applications that involve releases of hazardous pollutants in urban environments is rapidly increasing, therefore evaluation studies like that presented in this paper are of particular relevance. Wind tunnel experimental data sets present the additional advantage of containing much less atmospheric variability than field trials, which makes them very useful for the evaluation of Reynolds-averaged Navier-Stokes equations models, such as the one used in this study.

## METHODOLOGY

### Wind Tunnel Experiments

Wind tunnel experiments were conducted in the dispersion modelling wind tunnel of the Building Research Establishment, at Cardington. The wind tunnel has a working section 1.5 m high, 4.3 m wide and 22 m long. The value of the aerodynamic roughness length ( $z_0$ ) for these experiments was approximately 2.4 mm. The velocity of the approach flow at obstacle height was  $1.67\text{m}^3\text{ s}^{-1}$ . A detailed description of the wind tunnel and of the wind tunnel flow and dispersion characteristics is provided by Hall *et al.* (1996) and Mavroidis (1997). The obstacles examined in the present paper are a cube of height  $H=0.15\text{m}$  and a right cylinder of height  $H$  and diameter  $D=0.15\text{m}$ .

A single tracer gas source was used consisting of 47% methane in argon (to produce a neutrally buoyant release). Gas samples were drawn down small bore tubing through 20-port sampling valves into Flame Ionisation Detectors (FIDs), with a response time of approximately 0.3 s. Three detectors and sampling valves were used for the tracer gas measurements. A fourth FID permanently sampled the background concentration of the tracer, and the background level was subtracted from the measured concentration in the plume. Concentration detectors were placed at several locations downwind of the obstacle, both on the ground and at half the building height. The main source locations investigated here are: (a) 2 obstacle heights upwind, on the centreline and at half the building height (b) at the centre of the upwind face, (c) at the centre of the roof, and (d) at the centre of the downwind face of the obstacle. The main experimental configuration involving the cube and one of the source locations is presented in Figure 1.

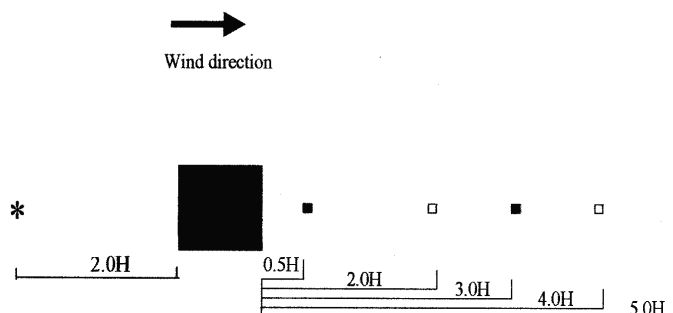


Figure 1. Plan view of the basic experimental configuration involving a single cube, with the source located  $2.0H$  upwind (\*: source, ■: detectors).

### Modelling Approach

The computational fluid dynamics code ADREA-HF, developed by the Environmental Research Laboratory, has been used for the simulations presented in this article. The purpose of ADREA-HF is to simulate the dispersion of buoyant or passive pollutants over complex geometries. ADREA-HF is a finite volumes code that solves the Reynolds-averaged equations for the mixture mass, momentum, energy, pollutant mass fraction and the variance of the pollutant mass fraction. Turbulence closure is obtained through the eddy viscosity concept, which, in the simulations presented in this paper, is calculated by the standard  $k-\varepsilon$  model. The turbulent kinetic energy  $k$  and the dissipation rate  $\varepsilon$  are calculated by transport equations. For the pollutant concentration variance, a three-dimensional transport equation is also solved. Details on the modelling approach regarding the concentration variance are included in Andronopoulos *et al.* (2002). The experimental characteristics of the source and the physical properties of the two gases were used for the simulations. The atmospheric stability conditions were taken as neutral for all modelled cases. The computed concentrations and concentration fluctuations were non-dimensionalised, to be directly comparable with the experimental data (Mavroidis, 1997; Mavroidis *et al.*, 2003).

### RESULTS AND DISCUSSION

In Figures 2 – 5 contour plots of calculated non-dimensionalised concentration are presented for all the cases simulated in this paper. The contour plots are drawn on the horizontal plane located at half the obstacle height  $H$ . It is observed that the plume is bifurcated around the obstacle in all cases except when the gas source is located in the downwind face of the cube and on the top of the cube. It is also noted that the bifurcation is more pronounced in the cases with the right cylindrical obstacle than those with the cube. At the ground level (not shown here) similar contour patterns are obtained, with higher concentrations extending slightly further downwind. When the source is located at the downwind face of the obstacle, higher concentrations occur for a longer distance downwind of the obstacle. When the source is located on top of the cube (Figure 5), the plume is mixed by the recirculation zone in the lee of the obstacle and touches the ground immediately downwind.

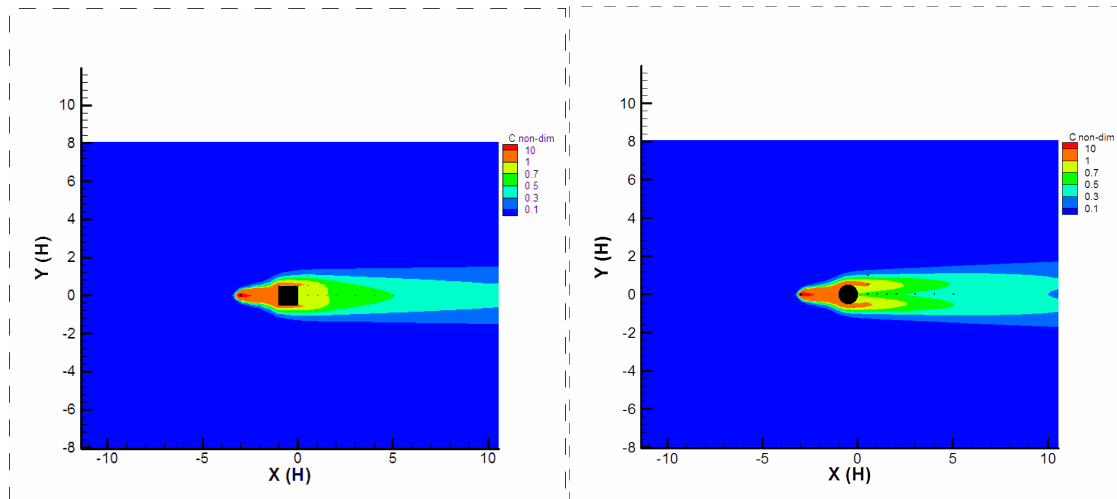


Figure 2. Contour plots of calculated non-dimensionalised concentration on the horizontal plane at the height of the gas source, located at a distance of  $2H$  upwind of the obstacle: cube (left), cylinder (right)

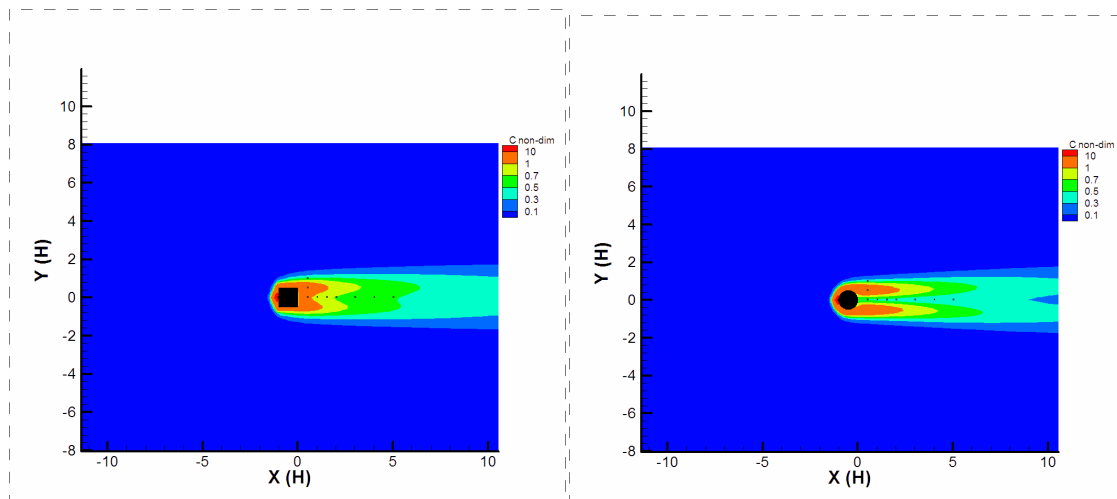


Figure 3. Contour plots of calculated non-dimensionalised concentration on the horizontal plane at the height of the gas source, located at the upwind face of the obstacle: cube (left), cylinder (right)

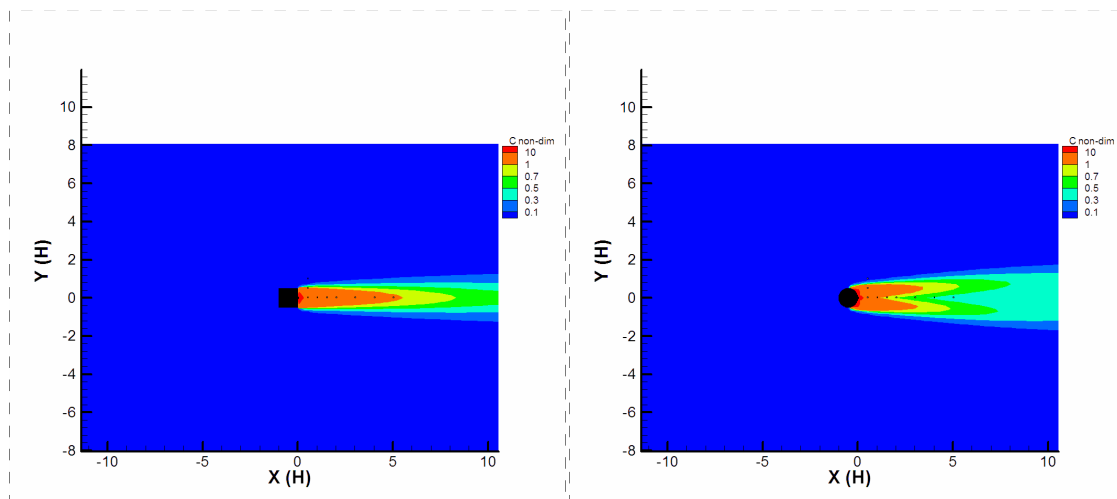


Figure 4. Contour plots of calculated non-dimensionalised concentration on the horizontal plane at the height of the gas source, located at the downwind face of the obstacle: cube (left), cylinder (right)

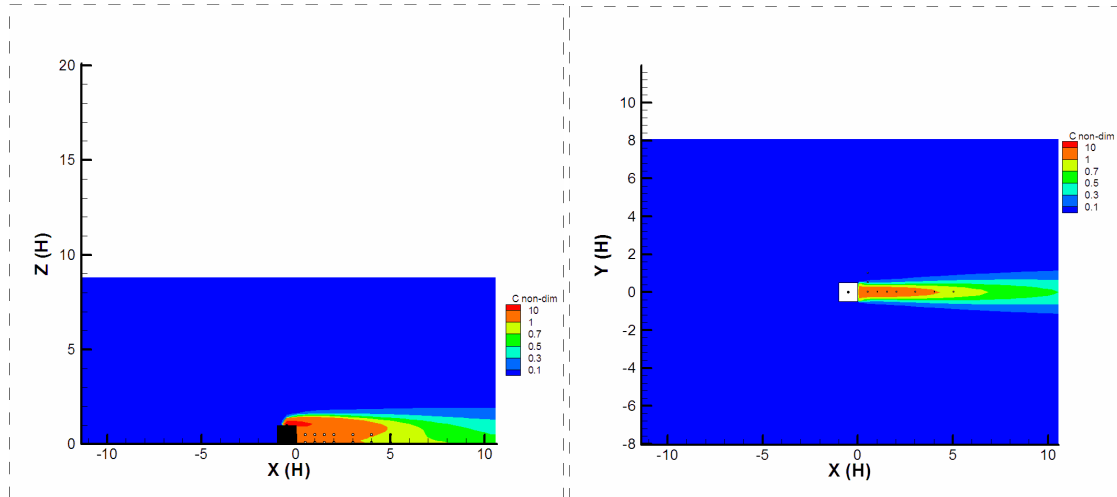


Figure 5. Contour plots of calculated non-dimensionalised concentration for the gas source located on top of the cubical obstacle: vertical plane (left), horizontal plane at the height of H/2 (right)

In Figures 6 and 7 the model’s results are compared to measurements for the cases with the gas source located 2H upwind of the cube and cylinder. Along-wind profiles of concentration and concentration fluctuation intensity (ratio of concentration standard deviation to concentration) downwind of the obstacle at the height of H/2 are plotted. The model fails to capture the high concentration values close to the obstacle, which are higher in the cube case, but further downwind the agreement is fairly good. The calculated fluctuation intensity initially increases and then levels out with downwind distance. The measured values exhibit a slight peak at 3H downwind distance both for the cube and cylinder that is not captured by the model. However the over-all calculated and measured fluctuation levels agree well for the cube case, while they are slightly over-estimated by the model for the cylinder case.

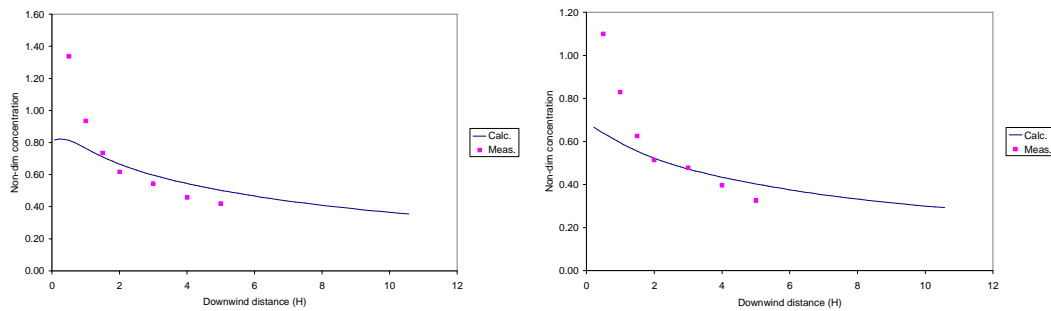


Figure 6. Comparison of calculated and measured non-dimensionalized concentration in the along-wind direction, downwind of the obstacle, at height H/2, for source located 2H upwind: Cube, (left), cylinder, (right)

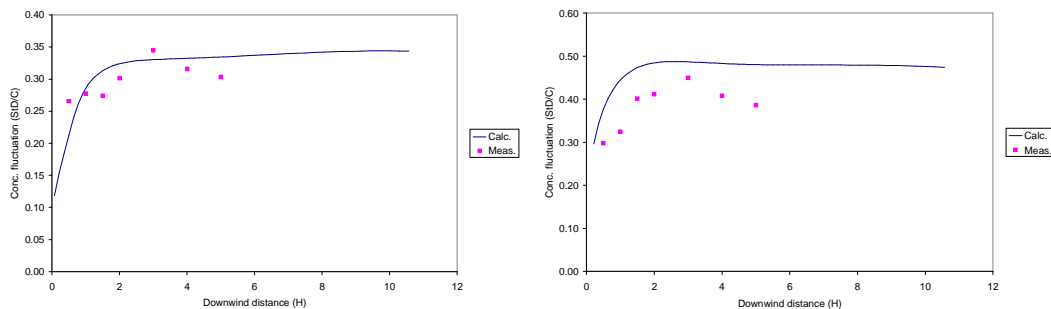


Figure 7. Comparison of calculated and measured concentration fluctuation intensity in the along-wind direction, downwind of the obstacle, at height H/2, for source located 2H upwind: Cube, (left), cylinder, (right)

In Figures 8 and 9 along-wind profiles are compared at the ground level for the cases with the source located at the downwind side of the obstacle. It appears that the model over-estimates concentrations for the cube at all distances, while for the cylinder only close to the obstacle. The agreement for the concentration fluctuation intensity is better for the cube, with the small peak captured by the model, while for the cylinder the model tends to under-estimate the fluctuations. Further research is needed to quantify the effects on the observed differences of factors such as turbulence modelling, boundary conditions etc.

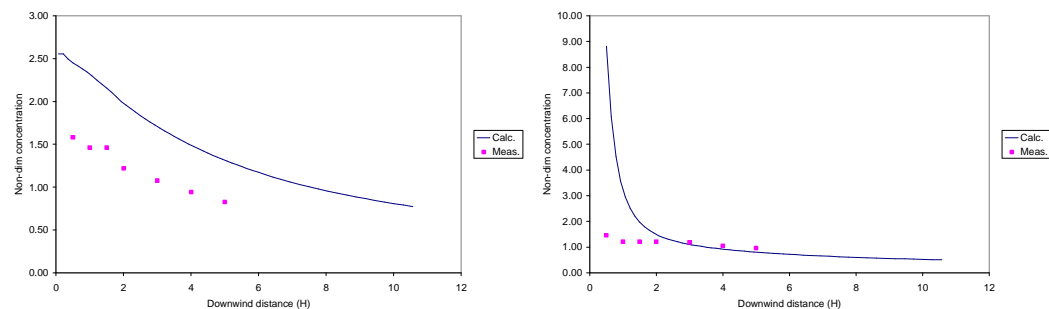


Figure 8. Comparison of calculated and measured non-dimensionalized concentration in the along-wind direction, downwind of the obstacle, at ground level, for source located at the downwind side: Cube, (left), cylinder, (right)

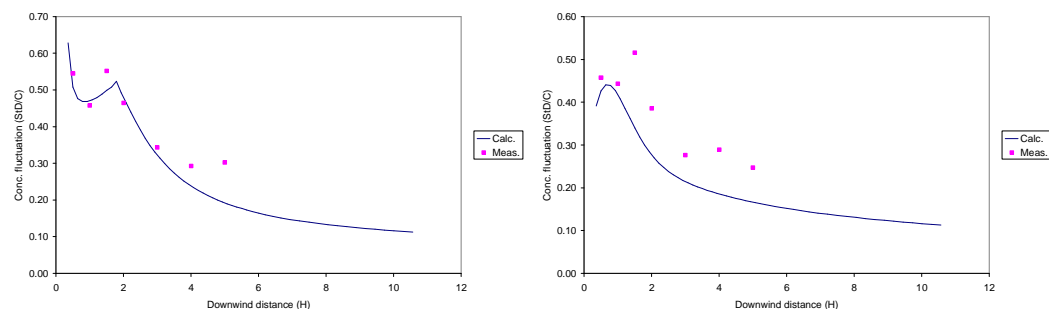


Figure 9. Comparison of calculated and measured concentration fluctuation intensity in the along-wind direction, downwind of the obstacle, at ground level, for source located at the downwind side: Cube, (left), cylinder, (right)

## CONCLUSIONS

Computational fluid dynamics (CFD) simulations of neutral gas dispersion wind tunnel experiments around isolated model buildings of cubical and cylindrical shapes are presented in this paper. Different gas source locations are examined. Patterns of computed concentration show a more pronounced plume bifurcation for the cases with the cylindrical obstacle. The model results for mean concentration and concentration fluctuation intensity are compared with measured data for model evaluation purposes, downwind of the obstacles at half the obstacle height and at ground level. The agreement is good for some cases, e.g., for the concentration at half the obstacle height and at distances 2 to 5 heights downwind, and poorer for others, such as e.g., the concentration close to the obstacles immediately downwind. Fluctuations intensity is predicted rather well overall. Further research will focus on quantifying the effects of factors such as turbulence modelling and boundary conditions on the level of agreement between model results and measurements in the wind tunnel.

## ACKNOWLEDGEMENTS

The field experiments simulated here were conducted with the support of the Atmospheric Dispersion Modelling Group at DSTL Porton Down, under agreement 2044/15/CBDE.

## REFERENCES

- Andronopoulos, S., Grigoriadis, D., Robins, A., Venetsanos, A., Rafailidis, S. and Bartzis, J.G., 2002: Three-dimensional modelling of concentration fluctuations in complicated geometry. *Environmental Fluid Mechanics*, 1, 415 – 440.
- Hall D.J., Macdonald R., Walker S., Spanton A.M., 1996: Measurement of dispersion within simulated urban arrays – A small scale wind tunnel study. BRE Report 178/96, Building Research Establishment, Watford, UK.
- Hosker R.P. Jr., 1984: Flow and diffusion near obstacles. Atmospheric Science And Power Production, (Ed. Randerson D.). Publication DOE/TIC 27601, National Technical Information Service, Springfield, Virginia, USA., 241-326.
- Mavroidis I., 1997: Atmospheric dispersion around buildings. Ph.D. Thesis, Environmental Technology Centre, Department of Chemical Engineering, UMIST, Manchester, UK.
- Mavroidis, I., Griffiths, R.F. and Hall, D.J., 2003: Field and wind tunnel investigations of plume dispersion around single surface obstacles. *Atmospheric Environment*, 37(21), 2903-2918.